A Two-Layer Optimization Framework for UAV Path Planning with Interval Uncertainties

Bai Li
School of Control Science and Engineering
Zhejiang University
Hangzhou, China
libai@zju.edu.cn

Raymond Chiong
School of Design, Communication and Information Technology
The University of Newcastle
Callaghan, Australia
Raymond.Chiong@newcastle.edu.au

Mu Lin
College of Biomedical Engineering and Instrument Science
Zhejiang University
Hangzhou, China
linmudl@zju.edu.cn

***Abstract*—We propose a two-layer optimization framework for the unmanned aerial vehicle path planning problem to handle interval uncertainties that exist in the combat field. When evaluating a candidate flight path, we first calculate the interval response (i.e., the upper and lower bounds) of the candidate flight path within the inner layer of the framework using a collocation interval analysis method (CIAM). Then, in the outer layer, we introduce a novel criterion for interval response comparison. The artificial bee colony algorithm is used to search for the optimal flight path according to this new criterion. Our experimental results show that the CIAM adopted is a feasible option, which largely eases the computational burden. Moreover, our derived flight paths can effectively handle bounded uncertainties without knowing the corresponding uncertainty distributions.**

Keywords—unmanned aerial vehicles; interval uncertainty; path planning; collocation interval analysis; optimization under uncertainty

I. INTRODUCTION

An unmanned aerial vehicle (UAV) refers to a generic aircraft design that operates with no human pilot onboard [1]. Due to their outstanding capability to work in remote or hazardous situations, UAVs have been widely used for many civil and military applications. Path planning, as a critical aspect in UAV flight missions, is about obtaining an optimal flight path from a starting point to a desired destination considering a variety of constraints in the combat field. Here, the optimality of a flight path can be represented by the minimized gross flight distance, fuel consumption, and exposure to radar or artillery, among others [2].

Conventional UAV path planning missions are usually focused on achieving optimality and/or reducing computational complexity. The handling of uncertainties that exist in the combat field, however, has often been neglected [3]. In such a context, it is important to carefully consider the environmental uncertainties when planning a UAV flight path. According to previous research studies, environmental uncertainties in a UAV path planning mission refer to inaccurate locations and unknown threat levels of hostile air defense weapons, outdated or unreliable terrain information, and so on [4-7]. Besides these, uncertainties can also arise from flight demands. To date, considerations on the latter are relatively rare. In this work, we consider both the environmental and mission demand uncertainties.

Typically, stochastic and fuzzy models have been used to describe and handle uncertainties. For stochastic programming, the uncertain coefficients are regarded as random variables and their probability distributions should be known. For fuzzy programming, the constraints and objective function are viewed as fuzzy sets and their membership functions need to be identified [8]. In both models, a correct membership function or probability distribution plays an important role to describe the uncertainties. However, it can be difficult to estimate a reliable membership function or a correct probability distribution function especially when the available information is scarce. In contrast, it is far easier to estimate the two bounds of an uncertain coefficient than to obtain the corresponding probability distribution [9]. This gives rise to new research directions in the area of uncertainty optimization, namely the interval analysis and interval number programming.

Interval numbers can be regarded as an extension of real numbers, or a non-fuzzy subset of the real axis with a precisely defined domain on it [10]. Interval number programming refers to transforming a programming problem with interval uncertainties to a deterministic one. In this process, efforts are needed to compare the candidate objective function "values". Here, the "values" are interval numbers rather than real numbers due to the interval uncertainties that exist in the problem. Many criteria have been proposed for interval number comparison [11-14]. Interval analysis, on the other hand, refers to obtaining an interval response to a candidate solution that is substituted into the objective function. Methods based on the Taylor expansion [15, 16] are common for interval analysis. Despite being efficient, the Taylor-based methods are limited to handling of uncertainties within small intervals because they depend on the first or second order sensitivity at the nominal points. To overcome this, an alternative called the collocation interval analysis method (CIAM) has been proposed [17]. The CIAM does not rely on sensitivity and thus works well when interval numbers are of large scale. Although a variety of applications of

978-1-4799-5375-2/14/$31.00 ©2014 IEEE

interval number programming or interval analysis exist (e.g., structure design, job shop scheduling, vital sign monitoring and fault detection), to the best of our knowledge, interval number based approaches have never been applied to handle uncertainties in a UAV path planning scheme. For UAV path planning, intelligence that can be utilized to estimate the distribution of uncertainties is generally insufficient due to the increasing complexity of the modern warfare. So, modeling the uncertainties using interval numbers is realistic and sensible.

In this paper, we propose a two-layer optimization framework for the UAV path planning scheme with interval uncertainties. In the inner layer, we calculate the interval response (i.e., the upper and lower bounds) for a candidate path using the CIAM. Then, in the outer layer, we define a novel criterion to locate the "optimal" interval number among all the candidate interval numbers through a search algorithm, namely the artificial bee colony (ABC) algorithm.

The remainder of this paper is organized as follows. In Section II, we introduce the basic cost function that serves as an evaluation of the flight path quality without any consideration of uncertainty. In Section III, we formulate a general interval number optimization problem concerning UAV flight path planning with uncertain interval coefficients. Then, in Section IV, we describe our novel criterion for interval number comparison. The overall structure of the two-layer framework is presented in Section V. After that, our experimental results together with the analyses are discussed in Section VI. Finally, the contributions of this work are summarized in Section VII.

II. THE FLIGHT COST FUNCTION

In this section, we define the basic flight cost function $F_{\text{cost}}(\mathbf{X})$, where $\mathbf{X}$ refers to a candidate flight path. Here, we preliminarily ignore the modeling of combat field uncertainties.

As the first step, we should explain how a flight path in a three-dimensional environment can be described through a matrix $\mathbf{X} = \begin{bmatrix} x_{11}, x_{12}, \ldots, x_{1D} \\ x_{21}, x_{22}, \ldots, x_{2D} \end{bmatrix}_{2\times D}$. Let us denote the starting point as S and the terminal point as T. First, we draw a segment ST connecting S and T. We denote $\mathrm{S^*T^*}$ as the projection of ST in the XOY plane (i.e., the plane determined by $Z=0$). After that, we divide $\mathrm{S^*T^*}$ into $(D+1)$ equal portions by a series of D parallel planes $Plane_k$ $(k=1,2,..,D)$ (see Figure 1). Each of the planes should be vertical to $\mathrm{S^*T^*}$ and parallel to the Z axis. Also, the intersection point between segment ST and each plane $Plane_k$ is identified as the original point in that plane. Thereafter, we can define two orthotropic axes LX_k, LY_k in $Plane_k$. Then, as is clearly shown in Figure 1, as many as $2D$ scalars can determine D points in the three-dimensional space. Including S and T at both ends, there should be $(D+2)$ points. A flight path can be formed if we connect those $(D+2)$ points in sequence. In this way, a matrix $\mathbf{X}_{2\times D}$ can determine a path with line segments from S to T [18]. In the remainder of this section, we focus on how to evaluate the quality of candidate paths.

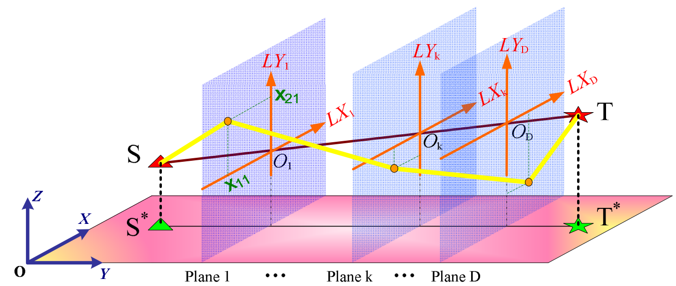

Figure 1. A schematic diagram of three-dimensional flight path description.

In a conventional UAV path planning mission without any uncertainty, a high-quality flight path refers to one with short gross flight length, low altitude, no probability of ground collision and good trajectory smoothness. In this work, we do not aim to establish a multi-objective optimization problem. Instead, we pursue for a synthetically low-cost path. Thus, we define our basic cost function as follows:

$$F_{\text{cost}} = w_1 \cdot C_{length} + w_2 \cdot C_{altitude} + w_3 \cdot C_{threat} + w_4 \cdot C_{collision} + w_5 \cdot C_{smooth}, \tag{1}$$

where C_{length} penalizes longer paths, $C_{altitude}$ penalizes paths with higher average altitudes, C_{threat} penalizes paths cutting through threatening zones (e.g., zones within the radar detection scope or ground weapon attack scope), $C_{collision}$ penalizes paths where collision to the ground occurs, and C_{smooth} penalizes paths that are not sufficiently smooth. $w_1 \sim w_5$ denote weight parameters according to a user's demand (e.g., if we set $w_1 = 0$, it implies that we do not worry about the flight length at all). Here, we use C_{length}, $C_{altitude}$ and C_{smooth} as optimization terms to improve the quality of the flight path. The other two terms, i.e., C_{threat} and $C_{collision}$, are flexibility terms reflecting whether a path is "flyable" or not. If there is no violation of these two fundamental restrictions, C_{threat} and $C_{collision}$ should equal 0. Otherwise, they range from P_{large} to $(P_{large}+1)$, where P_{large} is set to a large enough constant to guarantee that the cost function value of any feasible path will be smaller than any one path that is infeasible [2].

In this work, the term C_{length} that reflects the flight path length is defined as follows:

$$C_{length} = 1 - \frac{\overline{\mathrm{ST}}}{\widehat{\mathrm{ST}}}, \tag{2}$$

where $\overline{\text{ST}}$ denotes the length of segment ST, and $\widehat{\text{ST}}$ refers to the path length consisting of many line segments. Since the shortest distance between two points is always a straight line, we have $C_{length} \in [0,1]$.

The term $C_{altitude}$ that reflects the altitude of a flight path can be defined as:

$$C_{altitude} = \frac{A_{path} - h_{\min}}{h_{\max} - h_{\min}}, \tag{3}$$

where $h_{\max}$ is the upper limit of the elevation in the space of concern, $h_{\min}$ is the lower limit, and A_{path} is the average altitude of the flight path. We set $h_{\max}$ and $h_{\min}$ as the largest and smallest heights of the terrain respectively. Thus, we have $C_{altitude} \in [0,1]$.

The term associated with the entrance of threat zones C_{threat} is defined as:

$$C_{threat} = \begin{cases} 0, & \text{if } L_{\text{inside}} = 0 \\ P_{large} + \dfrac{L_{\text{inside}}}{\widehat{\text{ST}}}, & \text{if } L_{\text{inside}} > 0 \end{cases}, \tag{4}$$

where L_{inside} stands for the length of subsections within a flight path that crosses any of the threat zones. Therefore, $C_{threat} \in \{0\} \bigcup [P_{large}, P_{large}+1]$. We define the threat zones as cylindrical regions. Through overlapping multiple cylinders, one can also represent complex threat zones [2].

The term associated with ground collisions $C_{collision}$ can be defined as:

$$C_{collision} = \begin{cases} 0, & \text{if } L_{under} = 0 \\ P_{large} + \dfrac{L_{under}}{\widehat{\text{ST}}}, & \text{if } L_{under} > 0 \end{cases}, \tag{5}$$

where L_{under} refers to the total length of subsections within a flight path that goes below the ground level (i.e., crashes to the ground). Like C_{threat}, we have $C_{collision} \in \{0\} \bigcup [P_{large}, P_{large}+1]$.

The term associated with path smoothness C_{smooth} can be defined as:

$$C_{smooth} = \frac{\sum_{i=1}^{D} \theta_i}{D \cdot \pi/2}, \tag{6}$$

where $\theta_i \in \left[0, \pi/2\right]$ denotes the intersection angle between the ith and $(i+1)$th subsections in the candidate flight path $(i = 1, 2, ..., D)$. Here, $C_{smooth} \in [0,1]$.

In order to compute the aforementioned A_{path}, L_{inside} and L_{under}, we first generate as many as Nfe sample points uniformly along each of those $(D+1)$ line segments. In this way, we can derive $\left(D+2+(D+1)\cdot Nfe\right)$ uniformly distributed sample points along the whole flight path. Taking the calculation of L_{inside} as an example, if n out of the $\left(D+2+(D+1)\cdot Nfe\right)$ sample points fall within the threat zones, we estimate L_{inside} as $\dfrac{n \cdot \widehat{\text{ST}}}{D+2+(D+1)\cdot Nfe}$. Although this is not exact, yet if we set Nfe large enough the approximation accuracy should be fine as well.

In brief, we have introduced how a flight path is determined through a matrix $\mathbf{X}_{2\times D}$ given the starting and terminal locations in this section. We have also shown how to calculate the cost $F_{\text{cost}}(\cdot)$ of the flight paths without considering uncertainties in the environment.

However, when the location or the detection scope of a hostile defending radar is not exactly known, such uncertainty does affect the output of the cost function and thus should not be ignored. In the subsequent sections, we will focus on how optimization can be done when interval uncertainties exist in the UAV path planning mission.

III. PROBLEM FORMULATION

A general interval number optimization problem regarding UAV flight path planning with uncertain interval coefficients can be stated as follows:

$$\min = F_{\text{cost}}(\mathbf{X}, \mathbf{Y}),\ \forall \mathbf{Y} \tag{7}$$

where $\mathbf{X} \in \mathbb{R}^{2\times D}$ refers to the parametric matrix that determines a flight path in the three-dimensional space, and $\mathbf{Y} \in \mathbb{R}^{1\times M}$ is a vector, of which each dimension can be an interval number. In this work, the elements in $\mathbf{Y}$ can be classified into two categories: one category refers to the uncertain locations and radii of the air defense weapons on the ground, while the other category denotes the user-specific weights $w_1 \sim w_5$ in the basic flight cost function (i.e., Eq. (1)).

For each specific $\mathbf{X}$, since $\mathbf{Y}$ covers multiple possibilities, the output "value" of the objective cost function $F_{\text{cost}}(\cdot)$ will not be a real number, but an interval number ranging from $\min_{\mathbf{Y}}\left(F_{\text{cost}}(\mathbf{X},\mathbf{Y})\right)$ to $\max_{\mathbf{Y}}\left(F_{\text{cost}}(\mathbf{X},\mathbf{Y})\right)$. We call such an interval number the "interval response".

When evaluating the quality of each candidate path $\mathbf{X}$, as a preliminary step, we need to do optimization according to $\mathbf{Y}$ in the inner layer to calculate its interval response. The first issue we aim to overcome being that this will lead to a two-nested optimization process and hence reduce the computational efficiency significantly [19]. The second issue is how we can compare among the interval responses so that the "optimal" one can be located? In other words, what kind of criterion should we use to sort the interval responses? The third issue concerns how to search for the optimal interval response in the outer layer under the given criterion.

In this work, we use the CIAM to solve the first issue. Compared to well-adopted interval analysis methods based on the Taylor expansion, the CIAM is a good non-gradient algorithm using several collocation points to improve the approximation accuracy [17, 19]. Also, we use the ABC algorithm to address the third issue. ABC algorithms have been confirmed to possess competitive advantages compared to some other swarm intelligence and evolutionary algorithms [20]. The details of the CIAM and ABC algorithm are not included in this paper due to space constraints. Interested readers should refer to [17] and [21] for details. We will tackle the second issue in the next section.

IV. Interval Number Comparison

In this section, we first review the criteria for interval number comparison. Then, we introduce our proposed novel criterion in detail.

A. Related work

Here, we denote lb_A and ub_A as lower and upper bounds of an interval number $\widetilde{A}$ respectively, i.e., $\widetilde{A}=[lb_A, ub_A]$. According to [22], one can compare two interval numbers only when:

$$\widetilde{A} \le \widetilde{B} \Leftrightarrow ub_A \le lb_B. \tag{8}$$

Ishibuchi and Tanaka proposed a criterion to compare between two overlapping intervals [11]. In their work, an order relation $\le_{\mathrm{LR}}$ is defined between $\widetilde{A}$ and $\widetilde{B}$:

$$\widetilde{A} \le_{\mathrm{LR}} \widetilde{B} \Leftrightarrow lb_A \le lb_B,\ ub_A \le ub_B. \tag{9}$$

The order relation $\le_{\mathrm{LR}}$ defines that if both the lower and upper limits of an interval are higher than that of another interval, then the former is of higher value than the latter.

In a similar way, Ishibuchi and Tanaka suggested another order relation $\le_{\mathrm{mw}}$ as follows:

$$\widetilde{A} \le_{\mathrm{mw}} \widetilde{B} \Leftrightarrow \frac{lb_A+ub_A}{2} \le \frac{lb_B+ub_B}{2},\ ub_A-lb_A \ge ub_B-lb_B. \tag{10}$$

The order relation $\le_{\mathrm{mw}}$ defines that if the central value of an interval is higher than that of another interval and if the latter is broader, then the former is said to be preferred if the problem is to choose the maximum of the two.

A series of extended criteria for comparison originating from the two aforementioned order relations exist [13, 23]. The details of these are not presented due to space constraints.

As an alternative, using probabilistic concepts, Nakahara et al. [24] defined the probability of interval inequality $\mathrm{Prob}(\widetilde{A} \le \widetilde{B})$ as follows:

$$\mathrm{Prob}(\widetilde{A} \le \widetilde{B}) = \mathrm{Prob}(a \le b), \tag{11}$$

where a and b are random variables uniformly distributed on $\widetilde{A}$ and $\widetilde{B}$ respectively and $\mathrm{Prob}(\widetilde{A} \le \widetilde{B})$ is the conventional probability of $a \le b$. The probability $\mathrm{Prob}(\widetilde{A} \le \widetilde{B})$ with all the six possible position relations between $\widetilde{A}$ and $\widetilde{B}$ on the real axis considered in general can be defined as:

$$\mathrm{Prob}(A \le B) = \frac{(vv-ww)(ub_B - \frac{vv+ww}{2})}{(ub_A-lb_A)(ub_B-lb_B)} + \frac{ww-lb_A}{ub_A-lb_A}, \tag{12}$$

where

$$ww = \min\{\max\{lb_A, lb_B\}, ub_A\},$$

$$vv = \max\{\min\{ub_A, ub_B\}, lb_A\}.$$

B. Issues to be considered

Considering the criteria for interval number comparison discussed, we believe that only Eq. (8) holds true constantly. The others can cause some specific kinds of problems.

An adverse case regarding Eqs. (9) and (10) is raised in Figure 2, where both $\le_{\mathrm{LR}}$ and $\le_{\mathrm{mw}}$ relations are satisfied, but the true probability density functions (PDFs) indicate the opposite. Through this example, we would like to emphasize that, even though we do not know and do not expect to know the true PDFs of two interval numbers when comparing them, it by no means implies that we should ignore the PDFs or fabricate two PDFs for them. In regard to the criterion shown in Eq. (12), only when $\widetilde{A}$ and $\widetilde{B}$ obey the uniform distribution will its correctness be guaranteed. However, the core characteristic of the interval number theory should be non-probabilistic, and this was largely ignored by previous studies. Therefore, we believe that no direct comparison conclusion can be drawn when two interval numbers overlap with the other. Given an uncertain coefficient, we are not able to acquire a reliable uncertainty distribution. What we can know for sure is that there *exists* the possibility that such a bounded uncertain coefficient can reach every position in an interval.

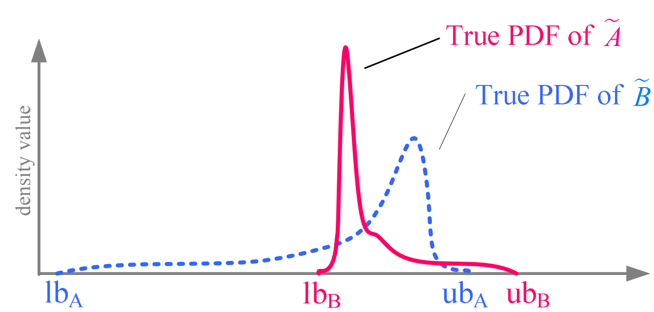

Figure 2. An example revealing the inefficiency of both $\le_{\mathrm{LR}}$ and $\le_{\mathrm{mw}}$ relations as defined in Eqs. (9) and (10) respectively. Although $\widetilde{A} \le_{\mathrm{LR}} \widetilde{B}$ and $\widetilde{A} \le_{\mathrm{mw}} \widetilde{B}$ both hold true, according to the true PDFs, one can see that $\widetilde{B}$ is more likely to be smaller than $\widetilde{A}$.

In the next sub-section, we introduce our new criterion to more robustly compare two interval numbers.

C. A novel criterion for interval number comparison

For the convenience of presentation, here we argue that $[lb_0, ub_0]$ equals an interval response, i.e.,

$$[lb_0, ub_0] = \left[\min_{\mathbf{Y}}\left(F_{\text{cost}}(\mathbf{X}_0, \mathbf{Y})\right), \max_{\mathbf{Y}}\left(F_{\text{cost}}(\mathbf{X}_0, \mathbf{Y})\right)\right].$$

First, we temporarily regard $\mathbf{X}$ and $\mathbf{Y}$ (in Eq. (7)) as free variables, and then minimize $F_{\text{cost}}(\mathbf{X}, \mathbf{Y})$ to obtain $\min_{\mathbf{X},\mathbf{Y}}\left(F_{\text{cost}}(\mathbf{X}, \mathbf{Y})\right) = val_{\min\min}$. After that, we take only $\mathbf{X}$ as a free variable, with the aim to find the very $\mathbf{Y}$ that makes $F_{\text{cost}}(\mathbf{X}, \mathbf{Y})$ largest. This means we need to obtain $\min_{\mathbf{X}}\left(\max_{\mathbf{Y}}\left(F_{\text{cost}}(\mathbf{X}, \mathbf{Y})\right)\right) = val_{\min\max}$. Now, we can safely conclude that $lb_A \geq val_{\min\min}$ and $ub_A \geq val_{\min\max}$.

Our poposed criterion is as follows:

$$obj(lb_0, ub_0) = \left(1 - \frac{val_{\min\max}}{ub_0}\right) + weight \cdot \left(\frac{ub_0 - val_{\min\max} + \varepsilon}{lb_0 - val_{\min\min} + \varepsilon}\right), \quad (13)$$

where ε is a small positive number for avoiding the denominator/numerator of the second term to be zero.

As can be seen, $obj(lb_0, ub_0)$ is a weighted sum of two items. The first item is $\left(1 - \frac{val_{\min\max}}{ub_0}\right)$, which ranges from 0 to 1. In the UAV flight path planning problem, it is essential to guarantee that the computed route covers all the uncertainties (especially the worst case). Since ub_0 reflects the worst case (i.e., the one with the largest cost function value for $\mathbf{X}_0$), we use such ub_0 in our criterion for a conservative design. The second term (i.e., $\frac{ub_0 - val_{\min\max} + \varepsilon}{lb_0 - val_{\min\min} + \varepsilon}$) reflects robustness. Broadly speaking, the length of an interval number (i.e., $(ub_0 - lb_0)$) can reflect the volatility. However, in order to measure such volatility, we do not simply use the absolute distance between two bounds (i.e., $(ub_0 - lb_0)$). Instead, we do something like $(ub_0 - lb_0)/lb_0$. At this point, when lb_0 is smaller, the numerator $(ub_0 - lb_0)$ will be relatively larger (and vice versa). For example, $(100-50)/50$ is smaller than $(51-1)/1$. This is because the change rate of the former interval solution (i.e., $[50,100]$) is lower than the latter one (i.e., $[1,51]$).

By tuning the user-specific parameter *weight* we are able to strike a balance between the two terms (conservatism and robustness), which, in turn, allowing us to find the interval solution that is optimal.

V. The Overall Structure

In this section, we present the step-by-step procedures of our two-layer optimization framework for UAV path planning with interval uncertainties.

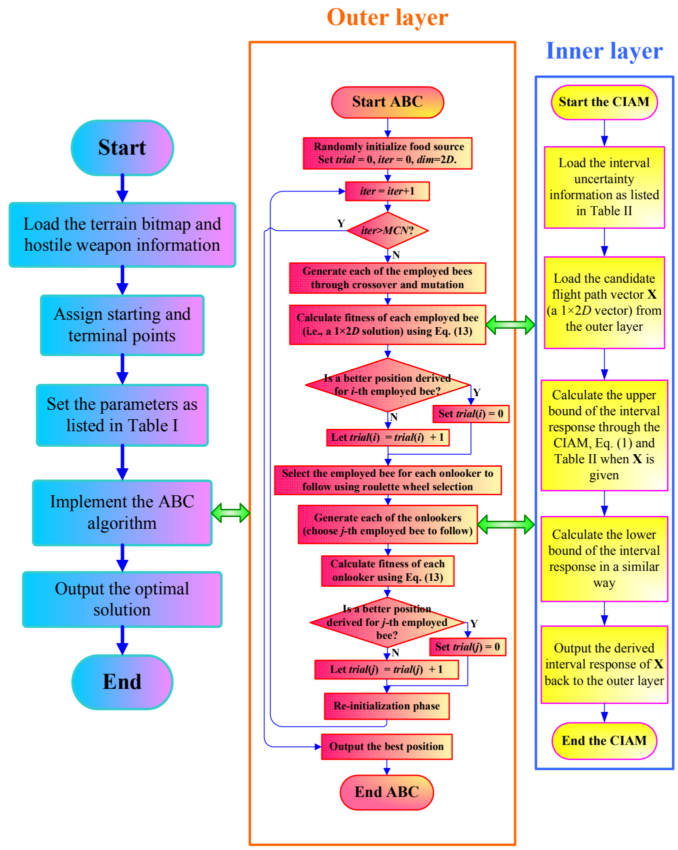

Figure 3. The flowchart of our two-layer optimization framework.

Step 1. Load combat field situations (i.e., a 159×199 terrain bitmap and hostile weapon intelligence). Allocate starting and terminal points in the combat field.

Step 2. Set parameters D, Nfe, SN, MCN, $Limit$, $P_{l\arg e}$, r, q and $weight$ as listed in Table I.

Step 3. Set the upper and lower bounds for $\mathbf{X}_{1\times 2D}$ (i.e., $\mathbf{X}_{\text{lb}} \leq \mathbf{X} \leq \mathbf{X}_{\text{ub}}$). Reshape every solution matrix $\mathbf{X}_{2\times D}$ to a single-row vector $\mathbf{X}'_{1\times 2D}$. Reshape the upper and lower bounds $\mathbf{X}_{\text{lb}}$ and $\mathbf{X}_{\text{ub}}$ to single-row vectors, then $\mathbf{X}'_{\text{lb}} \leq \mathbf{X}' \leq \mathbf{X}'_{\text{ub}}$.

Step 4. Generate the upper and lower bounds for each element in the uncertain variable $\mathbf{Y} = [y_1, y_2, \ldots, y_M]_{1\times M}$ according to combat field information.

Step 5. Execute the ABC algorithm in the outer layer to search for the optimal flight path according to the criterion in Eq. (13). To this end, when the quality of a candidate solution $\mathbf{X}$ is to be evaluated, the CIAM is needed to compute the corresponding interval response in the inner layer.

Step 6. Terminate the execution of the ABC algorithm when the iteration number reaches MCN .

Step 7. Output the current best flight path. Then, end the framework execution.

A schematic flowchart of the two-layer optimization framework is shown in Figure 3.

VI. Experiments and Results

We have systematically conducted a series of simulation experiments, first to investigate the performance of the CIAM used in the inner layer, and then the proposed criterion as well as the overall framework. All the simulations were carried out in a Matlab R2014a environment and executed on a 6-core Intel Xeon CPU with 64 GB RAM running at 6×3.06 GHz under Mac OS X 10.9 Mavericks.

Parameter settings are listed in Table I. We also set $w_1 \in [1.2, 2]$, $w_2 \in [0.8, 1.25]$ and $w_3 = w_4 = w_5 = 1$ for Eq. (1). In this work, the interval uncertainties lie in the central locations and detection radii of the threats (as listed in Table II), as well as two weights (i.e., w_1 and w_2) in Eq. (1). The aforementioned two bounds of $\mathbf{X}_{2\times D}$ were set as $\mathbf{X}_{\text{lb}} = \begin{bmatrix} -40 & \cdots & -40 \\ -100 & \cdots & -100 \end{bmatrix}_{2\times D}$ and $\mathbf{X}_{\text{lb}} = \begin{bmatrix} 40 & \cdots & 40 \\ 200 & \cdots & 200 \end{bmatrix}_{2\times D}$.

TABLE I
Parameter Settings for the Experiments

Parameter	Description	Setting
D	number of planes between S and T	-
Nfe	number of finite elements along each subsection	15
P_{large}	a constant in Eqs. (4) and (5)	100
Dim	dimension of solution in ABC	equals $2D$
MCN	maximal cycle number in ABC	-
SN	swarm population in ABC	20
$Limit$	a threshold regarding re-initialization in ABC	equals Dim
$weight$	weight in our novel criterion	1
q	number of truncation terms in the CIAM	10
r	number of Gauss integral points in the CIAM	5
S	staring point in the combat field	(1, 159, 277)
T	terminal destination in the combat field	(198, 4, 52)

TABLE II
Interval Uncertainty Information in the Threats

Threat No.	Threat Center Location in Horizontal Axis	Threat Center Location in Vertical Axis	Threat Radius
1	98	[38,40]	[10,11]
2	[98,101]	[78,80]	[10,11]
3	[118,120]	98	10
4	[138,140]	[28,30]	[10,11]
5	[168,171]	[58,60]	[9,11]
6	[133,135]	[63,65]	[10,11]
7	168	[98,100]	[9,10]
8	[158,160]	[128,130]	10

In the first set of experiments, we investigated the performance of the CIAM by comparing it with the ABC algorithm as well as a gradient-based optimization method called interior point optimization (IPOPT). Besides the settings in Table I, here we set $MCN = 50$ and $D = 10$. We randomly generated 40 feasible flight paths and computed the corresponding interval response for each of them by means of the three methods in comparison (i.e., the CIAM, ABC and IPOPT). The results are shown in Figures 4 and 5. The corresponding time consumptions are plotted in Figure 6. In addition, we performed the Wilcoxon rank-sum test (at a significance level of $\alpha = 0.05$) to verify the statistical differences between the results obtained.

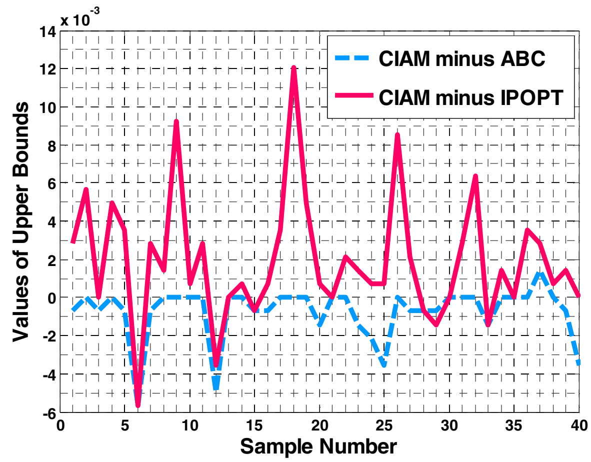

Figure 4. Differences of the computed upper bounds by means of the CIAM, ABC and IPOPT. The solid line represents the upper bounds derived by the CIAM minus those derived by IPOPT. The dashed line represents the upper bounds derived by the CIAM minus those derived by ABC for each of the 40 samples. Note that the solid line is roughly above the horizontal axis, which implies that the CIAM has derived higher upper bounds than IPOPT.

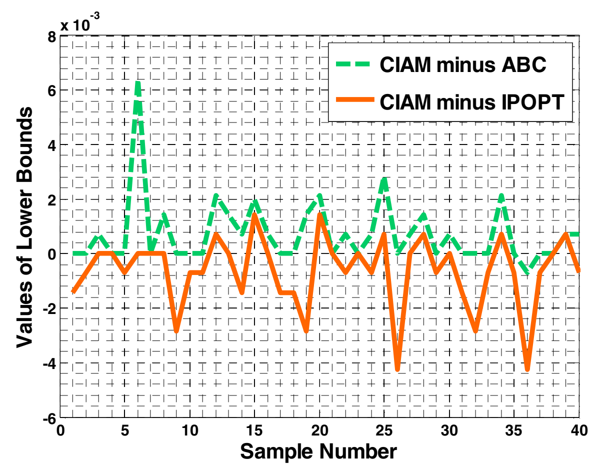

Figure 5. Differences of the computed lower bounds by means of the CIAM, ABC and IPOPT. The solid line represents the lower bounds derived by the CIAM minus those derived by IPOPT. The dashed line represents the lower bounds derived by the CIAM minus those derived by ABC for each of the 40 samples. Note that the solid line is roughly below the horizontal axis, which implies that the CIAM has derived smaller lower bounds than IPOPT.

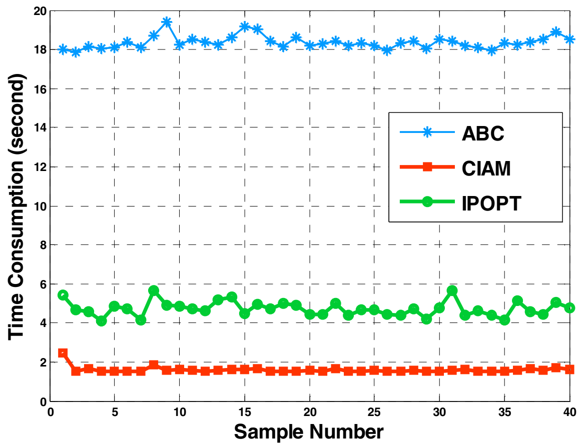

Figure 6. Time consumptions of the CIAM, ABC and IPOPT when tested on the 40 samples.

The simulation results illustrated in Figures 4, 5 and 6 confirm that: (1) the ABC algorithm significantly outperforms the other two; (2) the CIAM outperforms the gradient-based IPOPT with statistical significance; (3) the CIAM significantly outperforms the other two in time consumption; and (4) the time consumptions of the CIAM are more consistent (i.e., less fluctuating) than that of IPOPT or ABC. These findings indicate that the CIAM is a reasonable choice for calculating the interval responses in the inner layer.

In the second set of experiments, we investigated the efficacy of our proposed criterion for interval number comparison in Eq. (13). We compared it against three other commonly used criteria. The first one is defined as follows:

$$obj_{Criterion\_1}(lb_0, ub_0) = \frac{ub_0 + lb_0}{2}. \tag{14}$$

The second criterion refers to $obj_{Criterion\_2}(lb_0, ub_0) = lb_0$, while the third one can be defined as $obj_{Criterion\_3}(lb_0, ub_0) = ub_0$. It is interesting to note that optimization on the basis of the second criterion results in obtaining $val_{\min\min}$ while optimizing on the basis of the third criterion will obtain $val_{\min\max}$. Each optimal path under these criteria was obtained after 5000 iterations when using ABC in the outer layer ($D = 10$). Through the optimization of the second and third criteria, we obtained $val_{\min\min} = 0.98125$ and $val_{\min\max} = 1.57177$, which are parameter values that should be known in advance for our proposed criterion. In order to test these four criteria under different kinds of uncertainties, we designed two test cases, each includes 10,000 randomly generated combat situations. The samples in the first case follow a uniform distribution, while the samples in the second case obey a standard normal distribution (those out of bounds should be fixed at the bounds).

The results of the two cases are listed in Table III, where "Mean" denotes the average flight cost value of the 10,000 possibilities and S.D. is the corresponding standard deviation. From the results in the table, we can see that, among the four criteria, our proposed criterion leads to the lowest flight cost function values on average and its robustness is reflected by the S.D.

TABLE III
STATISTICAL TESTS ON THE RESULTS OF DIFFERENT CRITERIA FOR INVERTAL NUMBER COMPARISON

No.	Criterion 1		Criterion 2		Criterion 3		Eq. (13)	
	Mean	S.T.	Mean	S.T.	Mean	S.T.	Mean	S.T.
Case 1	1.411	0.123	6.070	21.336	1.300	0.114	**1.253**	**0.110**
Case 2	1.300	0.169	10.959	29.691	1.197	0.156	**1.153**	**0.151**

Before ending this section, we show the simulation results of our two-layer framework under the conditions of $MCN = 5000$ and $D = 10$ or 15. Figures 7 and 9 show the global view of the obtained paths. When observed in a local perspective (see Figures 8 and 10), it is clear that the obtained flight paths have successfully avoided entering the regions that fall within the scope of hostile weapon.

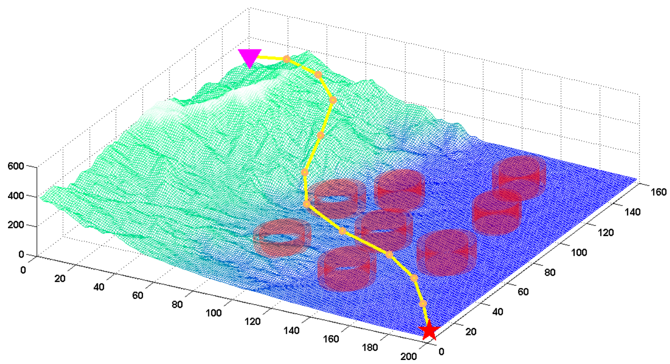

Figure 7. Global view of the computed flight path (when $D = 10$ and $MCN = 5000$).

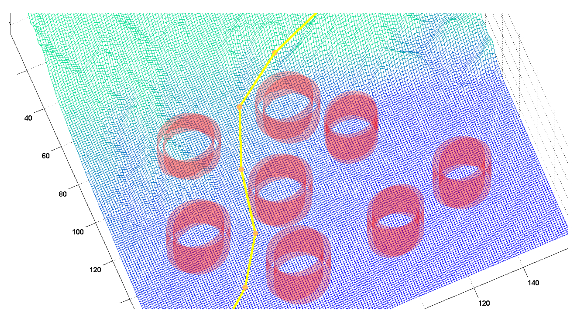

Figure 8. A local perspective based on the result from Figure 7.

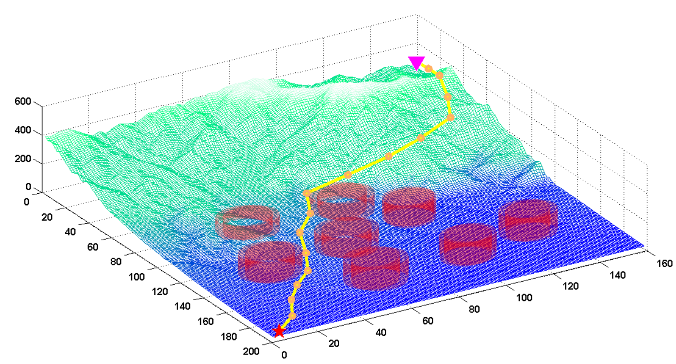

Figure 9. Global view of the computed flight path (when $D = 15$ and $MCN = 5000$).

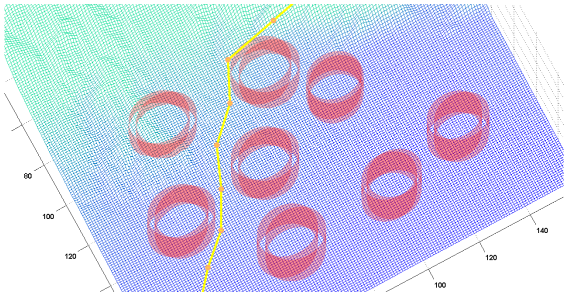

Figure 10. A local perspective based on the result from Figure 9.

VII. Conclusion

In this paper, we have presented a two-layer optimization framework to handle the interval uncertainties in UAV path planning. Our work has two important contributions. First, we have used the CIAM and estimated the interval responses in the inner layer of our framework successfully. Second, we have proposed a novel criterion for interval number comparison.

Despite the promising results, there is room for further improvement in the methods used for the framework (e.g., on time consumption). Future work will also consider more complicated cases.

Acknowledgment

We thank the four anonymous referees for their valuable comments and suggestions. The second author would like to acknowledge support from the University of Newcastle's Faculty of Science and Information Technology Strategic Initiatives Research Fund under Grant 1031415. This work is also supported in part by the 6th National College Students' Innovation & Entrepreneurial Training Program of China under Grant 201210006050.

References

[1] F. Nex, and F. Remondino, "UAV for 3D mapping applications: a review," *Applied Geomatics*, vol. 6, no. 1, pp. 1-15, 2014.

[2] V. Roberge, M. Tarbouchi, and G. Labonte, "Comparison of parallel genetic algorithm and particle swarm optimization for real-time UAV path planning," *IEEE Transactions on Industrial Informatics*, vol. 9, no. 1, pp. 132-141, 2013.

[3] K. Ok, S. Ansari, B. Gallagher, W. Sica, F. Dellaert, and M. Stilman, "Path planning with uncertainty: Voronoi uncertainty fields," *Proceedings of the International Conference on Robotics and Automation (ICRA 2013)*, IEEE, pp. 4596-4601, 2013.

[4] D. Rathbun, S. Kragelund, A. Pongpunwattana, and B. Capozzi, "An evolution based path planning algorithm for autonomous motion of a UAV through uncertain environments," *Proceedings of the 21st Digital Avionics Systems Conference*, pp. 1-12, 2002.

[5] R. Alterovitz, and K. Goldberg, "The stochastic motion roadmap: a sampling-based framework for planning with motion uncertainty," In *Motion Planning in Medicine: Optimization and Simulation Algorithms for Image-Guided Procedures*, R. Alterovitz, and K. Goldberg, Eds. Berlin: Springer-Verlag, pp. 75-89.

[6] M. Jun, and R. D'Andrea, "Path planning for unmanned aerial vehicles in uncertain and adversarial environments," *Cooperative Control: Models, Applications and Algorithms*, pp. 95-110, 2003.

[7] A. Pongpunwattana, and R. Rysdyk, "Real-time planning for multiple autonomous vehicles in dynamic uncertain environments," *Journal of Aerospace Computing, Information, and Communication*, vol. 1, no. 12, pp. 580-604, 2004.

[8] G. Klir, and B. Yuan, Eds. *Fuzzy Sets and Fuzzy Logic*. New Jersey: Prentice Hall, 1995.

[9] A. Sengupta, T. K. Pal, and D. Chakraborty, "Interpretation of inequality constraints involving interval coefficients and a solution to interval linear programming," *Fuzzy Sets and Systems*, vol. 119, no. 1, pp. 129-138, 2001.

[10] A. Sengupta, and T. K. Pal, "On comparing interval numbers: a study on existing ideas," In *Fuzzy Preference Ordering of Interval Numbers in Decision Problems*, A. Sengupta, and T. K. Pal, Eds. Berlin: Springer-Heidelberg, pp. 25-37.

[11] H. Ishibuchi, and H. Tanaka, "Multiobjective programming in optimization of the interval objective function," *European Journal of Operational Research*, vol. 48, no. 2, pp. 219-225, 1990.

[12] Y. Yao, "Interval-set algebra for qualitative knowledge representation," *Proceedings of the Fifth International Conference on Computing and Information (ICCI 1993)*, IEEE, pp. 370-374, 1993.

[13] S. Okada, and M. Gen, "Order relation between intervals and its application to shortest path problem," *Computers and Industrial Engineering*, vol. 25, no. 1-4, pp. 147-150, 1993.

[14] Q. Zhang, Z. Fan, and D. Pan, "A ranking approach for interval numbers in uncertain multiple attribute decision making problems," *Systems Engineering-Theory & Practice*, vol. 19, no. 5, pp. 129-133, 1999 (in Chinese).

[15] Z. Qiu and X. Wang, "Comparison of dynamic response of structures with uncertain-but-bounded parameters using non-probabilistic interval analysis method and probabilistic approach," *International Journal of Solids and Structures*, vol. 40, no. 20, pp. 5423-5439, 2003.

[16] Z. Wang and X. Qiu, "Interval finite element analysis of wing flutter," *Chinese Journal of Aeronautics*, vol. 21, no. 2, pp. 134-140, 2008.

[17] W. Qi and Z. Qiu, "A collocation interval analysis method for interval structural parameters and stochastic excitation," *Science China Physics, Mechanics and Astronomy*, vol. 55, no. 1, pp. 66-77, 2012.

[18] B. Li, L. G. Gong and C. Zhao, "Unmanned combat aerial vehicles path planning using a novel probability density model based on artificial bee colony algorithm," *Proceedings of the Fourth International Conference on Intelligent Control and Information Processing (ICICIP 2013)*, IEEE, pp. 620-625, 2013.

[19] Z. Qiu and W. Qi, "Non-probabilistic reliability-based structural design optimization based on the interval analysis method," *Science China Physics, Mechanics and Astronomy*, vol. 43, no. 1, pp. 9, 2013.

[20] D. Karaboga, B. Gorkemli, C. Ozturk and N. Karaboga, "A comprehensive survey: artificial bee colony (ABC) algorithm and applications," *Artificial Intelligence Review*, vol. 42, no. 1, pp.21-57, 2014.

[21] B. Li, R. Chiong and L. Gong, "Search-evasion path planning for submarines using the artificial bee colony algorithm," *Proceedings of the IEEE Congress on Evolutionary Computation (CEC 2014)*, IEEE, pp. 528-625, 2014.

[22] R. E. Moore, and F. Bierbaum, Eds. *Methods and Applications of Interval Analysis*. Philadelphia: SIAM, 1979.

[23] S. Chanas, and D. Kuchta, "Multiobjective programming in optimization of interval objective functions — a generalized approach," *European Journal of Operational Research*, vol. 94, no. 3, pp. 594-598, 1996.

[24] Y. Nakahara, M. Sasaki, and M. Gen, "On the linear programming problems with interval coefficients," *Computers and Industrial Engineering*, vol. 23, no. 1-4, pp. 301-304, 1992.